

The obscured γ -ray and UHECR universe

Charles D. Dermer

Code 7653, Naval Research Laboratory, 4555 Overlook Ave., SW, Washington, DC
20375-5352, USA

E-mail: dermer@ssd5.nrl.navy.mil

Abstract. Auger results on clustering of $\gtrsim 60$ EeV ultra-high energy cosmic ray (UHECR) ions and the interpretation of the γ -ray spectra of TeV blazars are connected by effects from the extragalactic background light (EBL). The EBL acts as an obscuring medium for γ rays and a reprocessing medium for UHECR ions and protons, causing the GZK cutoff. The study of the physics underlying the coincidence between the GZK energy and the clustering energy of UHECR ions favors a composition of $\gtrsim 60$ EeV UHECRs in CNO group nucleons. This has interesting implications for the sources of UHECRs. We also comment on the Auger analysis.

1. Introduction

The recent reports [1, 2] from the Pierre Auger Observatory collaboration of high-significance clustering of UHECRs along the supergalactic plane has opened multi-messenger astronomy. This advance is closely connected to progress in γ -ray and neutrino astronomy. Here we focus on new techniques to unravel the problem of UHECR origin in light of the Auger results. This topic is developed in more detail in my Mérida ICRC contribution [3] and in my book with Govind Menon [4].

2. Charged Particle Astronomy

We begin by reviewing the recent major results from Auger, including the discovery of the clustering of the arrival directions of UHECRs along the supergalactic plane [1]. This discovery was anticipated in the study by Stanev et al. [5], and we return to this paper in the discussion.

2.1. Pierre Auger Observatory

Auger is ~ 3000 km² in area, about the size of Rhode Island. It consists of 1600 shower detectors spaced 1.5 km apart, as well as four telescope enclosures each housing 6 telescopes to map Ni fluorescence. The directional point spread function of an UHECR is typically $\lesssim 1^\circ$. The original analysis published in *Science* [1] treated a data set from 1 Jan 2004 to 31 August 2007 consisting of 81 events with total energy $E > 40$ EeV.

2.2. Clustering Result

A probability statistic P corrected for exposure is constructed from the nearest-neighbor angular separation ψ between the arrival direction of an UHECR with energy E and the direction to AGN in the Véron-Cetty & Véron (VCV) catalog [6]. This catalog has 694 active galaxies with $z \leq 0.024$ or distance $d \lesssim 100$ Mpc (the total catalog has over 10^5 entries) but is incomplete,

especially around the plane of our Galaxy, and is also biased by different sample selection techniques.

In the Auger analysis [1], P was minimized for $\psi = 3.1^\circ$, threshold energy $E_{thr} = 56$ EeV, and $z_{max} = 0.018$ ($d_{max} = 75$ Mpc), containing 27 events (the two highest energy events were 90 and 148 EeV). Twelve events correlate within 3.1° of the selected $d < 75$ Mpc AGNs, and another three within the vicinity of one of these nearby AGN. By comparison, 3.2 events would be expected for an isotropic UHECR flux, which it clearly is not. Lack of correlation of $\gtrsim 60$ EeV UHECRs with the Galactic plane rules out Galactic (pulsar, stellar mass black hole) and Galactic halo (including halo dark matter annihilation) models, leaving extragalactic models viable, at least those that follow the matter distribution traced by the supergalactic plane like the nearby AGN in the VCV catalog.

The recent detailed Auger analysis [2] confirms these results, furthermore pointing out that the distance cutoff could range from $\sim 50 - 100$ Mpc and that $\psi \lesssim 6^\circ$. If one accepts the validity of these results, then *UHECRs with $E \gtrsim 60$ EeV originate from AGNs within $75(\pm 25)$ Mpc and are deflected in their travels by at most $\sim 3^\circ - 6^\circ$ by either the Galactic magnetic field [2] or the intergalactic magnetic field [3].*

The lack of a quasi-isotropic background UHECR flux above $E > E_{cl} \cong 60$ EeV is most simply explained if more distant UHECRs fail to arrive here at Earth. Because we know that there are sources of UHECRs with energy up to at least 300 EeV [7], it follows that unless we were in a unusual over-density of UHECR sources within ~ 100 Mpc and an under-density within $\sim 100 - 300$ Mpc or more, then energy losses of UHECRs accelerated by and injected from more sources more distant than $\approx 50 - 100$ Mpc are the cause of the Auger anisotropy.

The clustering energy $E_{cl} = 60$ EeV stands out in this analysis, separating $E \lesssim E_{cl}$ UHECRs formed mainly in the large scale quasi-homogeneous, isotropic universe at distance scales $d \gtrsim 50 - 100$ Mpc from the UHECRs formed in the clumpy structured universe at local, $d \lesssim 100$ Mpc scales.

2.3. GZK Cutoff

A high-significance steepening in the UHECR spectrum at the Greisen-Zatsepin-Kuzmin (GZK) [8, 9] energy $E_{GZK} \cong 10^{19.6}$ eV $\cong 4 \times 10^{19}$ eV was reported at the 2007 Mérida ICRC based on observations taken with the Auger Observatory [10] (see Figure 1), and earlier in 2007 by the HiRes collaboration [11] at $E_{GZK} \cong 10^{19.8}$ eV $\cong 6 \times 10^{19}$ eV.¹ This observation seems to confirm the prediction [8, 9] that interactions of UHECRs with CMBR photons will cause a break in the UHECR spectral intensity near 10^{20} eV. The coincidence $E_{GZK} \cong E_{cl}$ seems likely to originate from underlying physics.

2.4. UHECR Composition

The composition of UHECRs measured from $\approx 4.5 \times 10^{17}$ eV up to 4×10^{19} eV with Auger is neither dominant p nor Fe composition [12], and is not trending toward a lighter composition at the upper energy range, contrary to pre-Augur indications [13]. If the results of Ref. [12] can be extrapolated to $\gtrsim 60$ EeV, then ions must be included in the analysis unless the UHECR composition abruptly shifts to proton-dominated at $E \gtrsim E_{cl}$, as would be the case in neutral beam models of UHECRs [14].

3. GZK Energy

The energy of the GZK cutoff is not precisely defined. Returning to the classic paper by Greisen [8] for inspiration, let us work through the estimates in light of our new knowledge.

¹ The HiRes team also reports a significant dip structure at $E_{dip} \cong 10^{18.6}$ eV.

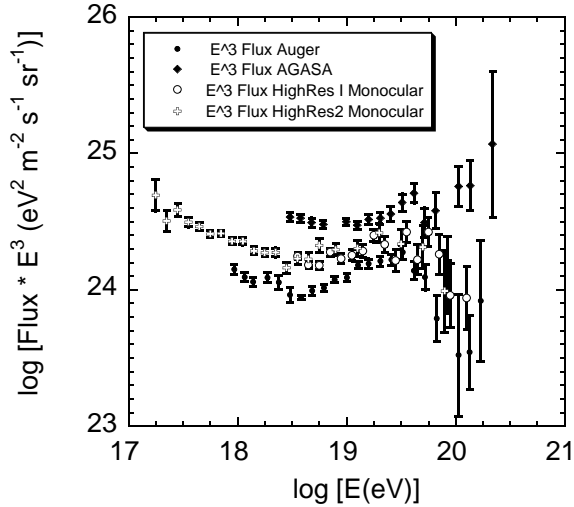


Figure 1. UHECR spectrum, plotted in the form of $E^3 I$, where I is the number intensity, for AGASA (filled diamonds), HiRes (open symbols), and Auger (filled circles).

3.1. GZK Energy: Analytic Analysis

UHECR protons with energy $E_p = \gamma_p m_p c^2 = 10^{20} E_{20}$ eV will undergo strong photopion losses when the threshold condition $\gamma_p \epsilon_{CMBR} \gtrsim m_\pi/m_e \cong 400$ is satisfied, where $\epsilon_{CMBR} \cong 2.70 \times 2.72 \text{ K}/5.9 \times 10^9 \text{ K} \cong 10^{-9}$ is the dimensionless mean photon energy, in units of the electron rest mass, of the CMBR. Strong photopion losses due to interactions with the peak energy photons of the CMB occur when $\gamma_p \gtrsim 4 \times 10^{11}$. The mean free path (MFP) for energy loss of a proton with energy $E_{20} \gtrsim 4$ is $\lambda_{\phi\pi} \cong (1/n_{CMBR} \sigma_{\phi\pi}) \cong 1/(400 \text{ cm}^{-3} \cdot 70 \mu\text{b}) \cong 10 \text{ Mpc}$. From a derivation using a step-function approximation for the product of photopion cross section and inelasticity [14], the mean-free-path for photopion energy losses of UHECR protons with CMBR photons is given by [3]

$$\lambda_{\phi\pi}(E_{20}) \cong \frac{13.7 \exp[4/E_{20}]}{[1 + 4/E_{20}]} \text{ Mpc} . \quad (1)$$

The values of $\lambda_{\phi\pi}(E_{20})$ for $E_{20} = 0.6, 0.8, 1,$ and 2 are $1400, 340, 150,$ and 35 Mpc , respectively. If the UHECR with energies between 60 and 100 EeV were protons, then they could originate over a large distance scale extending to 1 Gpc . This simple estimate suggests that the UHECRs cannot be protons because the Auger events originate from within 100 Mpc whereas the energy loss MFPs of UHECR protons at these energies are much greater.

Now we estimate the GZK MFPs of ions against photodisintegration on CMBR photons. Note that by contrast with UHECR protons, photopion losses of UHECR nucleons are not effective until $\gamma(\epsilon)_{CMB} \gtrsim m_\pi/m_e$ or $E_{20} \gtrsim 3A/(1+z)$, where A is the nucleon mass number. The pion-forming Δ resonance peak energy is $\cong m_e c^2 \epsilon_r \approx 300 \text{ MeV}$, a much higher energy than the giant dipole resonance (GDR) at $\approx 20 \text{ MeV}$, so photodisintegration breakdown usually dominates photopion losses for ions, especially for large A . The effective photodisintegration energy-loss rate for ions on the CMBR results from both GDR excitation with the emission of one and two nucleons, and from multi-nucleon breakup processes. Because the reaction is a threshold process and UHECRs with $E_{20} \ll 3A/(1+z)$ interact only with the Wien portion of the CMBR radiation field, the GDR is more important than multi-nucleon excitations for $E_{20} \sim 1$ UHECRs.

In this asymptote, we use the δ -function approximation for the photodisintegration cross section of nucleus A , namely

$$\sigma_A(\epsilon_r) \cong \frac{\pi}{2} \sigma_{0,A} \Delta_{GDR} \delta(\epsilon_r - \epsilon_{r,A}) , \quad (2)$$

[19, 20, 15], where

$$\sigma_{0,A} = 1.45A \text{ mb} , \quad \Delta_{GDR} \cong 15.6 , \quad \epsilon_{r,A} \cong 83.5A^{-0.21} ,$$

and $\epsilon_r = \gamma\epsilon(1 - \mu)$ is the invariant dimensionless photon energy in the ion's rest frame. In the δ -function approximation for the GDR, eq. (2), the derived inverse of the effective energy loss time scale of an UHECR ion due to photodisintegration processes with photons of the CMBR is

$$\begin{aligned} t_E^{-1}(E, A) &= \frac{2\pi^2 c \Delta_{GDR} k_A \epsilon_{r,A} \Theta}{\gamma^2 A \lambda_C^3} \ln([1 - \exp(-w_{r,A})]^{-1}) \\ &\cong 3.2 \times 10^{-15} \frac{k_A A^{1.79} (1+z)}{E_{20}^2} \ln \left[\frac{1}{1 - \exp(-w_{r,A})} \right] \text{ s} , \end{aligned} \quad (3)$$

where

$$w_{r,A} \equiv \frac{\epsilon_{r,A}}{2\gamma\Theta} = \frac{0.83A^{0.79}}{E_{20}(1+z)} .$$

The effective path length for photodisintegration in the δ -function approximation for the GDR is therefore

$$\lambda_E = \lambda_E(E, A) = ct_E(E, A) \rightarrow \frac{3.0E_{20}^2 \exp(0.83A^{0.79}/[(1+z)E_{20}])}{k_A A^{1.79}(1+z)} \text{ Mpc} \quad (4)$$

in the limit $w_{r,A} \gg 1$, that is, $E_{20} \ll 5(A/10)^{0.79}$.

When a single proton or neutron is ejected, then a fraction A^{-1} of the original energy E is lost to the original nucleon, and for the ejection of two nucleons, a fraction $2/A$ of energy is lost. For multi-nucleon injection, an average fractional energy loss k_A/A is used [17], where $k_A = 1.2/A, 3.6/A$, and $4.349/A$ for $A = 4, 10 \leq A \leq 22$, and $23 \leq A \leq 56$, respectively. The photodisintegration energy-loss MFPs have only a generalized meaning in terms of the mean distance for an UHECR nucleon to be broken up into mostly lower energy protons and neutrons and a nucleon with A about half of the original nucleonic mass. Photodisintegration of Fe, for example, leads to significant fraction of $A \lesssim 15$ nucleon secondaries [17].

Equating eq. (4) with an energy-loss distance $\lambda = 100\lambda_{100}$ for $E = 60E_{60}$ EeV gives $\exp(1.38A^{0.79}/E_{60})/[k_A A^{1.79}] = 333\lambda_{100}E_{60}^2$. It is easily verified that all nuclei with $A \gtrsim 14$ have energy-loss mean free paths at $E_{60} \approx 1$ much longer than 100 Mpc. On the basis of this analytic treatment, one might conclude UHECRs could originate only from nucleons with $4 \lesssim A \lesssim 14$.

3.2. GZK Energy: Numerical Analysis

These results are not conclusive unless additional radiation fields, including IR and optical features from stellar and reprocessed radiation, and energy-loss processes of photopair production and universal expansion are taken into account. Figure 2 shows the energy density of the EBL and cosmic rays, and the predicted upper limit to the cosmogenic neutrino energy density [21].

3.2.1. Extragalactic Background Light The mean intensity of light in intergalactic space is referred to as the EBL. The IR and optical EBL is decomposed at low redshift ($z \lesssim 0.25$) into a dust component and a stellar component as shown in Figure 3. These fits are assumed to span the likely range of the diffuse radiation fields between ≈ 1 and a few hundred μm at low z . The modified blackbody spectral energy density is written in the form

$$\epsilon u(\epsilon) = u_0 \frac{w^k}{\exp(w) - 1} = m_e c^2 \epsilon^2 n_{ph}(\epsilon) , \quad (5)$$

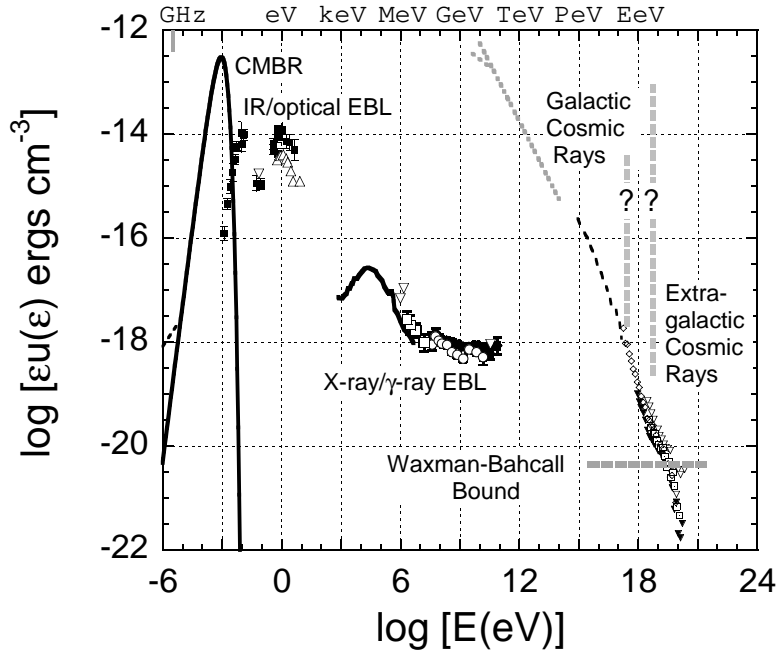


Figure 2. Energy density in intergalactic space of various radiations, including the CMBR, the IR and optical, X-ray, γ ray, extragalactic cosmic ray, and the predicted maximum energy density of cosmogenic neutrinos. Also shown is the near-Earth energy density of cosmic rays; the transition energy between the galactic and extragalactic component is uncertain.

Table 1. Properties of the Dust and Two Stellar Components

Component	$T(K)$	u_0 (10^{-14} ergs cm^{-3})	k
CMBR	2.72	6.38	4
Dust (Hi)	62	0.819	3.8
Dust (Low)	31	0.273	3.8
Star 1 (Hi)	7100	1.1	2.0
Star 1 (Lo)	7100	0.55	2.0
Star 2	16,600	0.5	3.0

where $w \equiv \epsilon/\Theta$. The stellar component is decomposed into the sum of two modified blackbodies, with the higher-temperature stellar component fixed. The HI EBL has the more intense dust and stellar fields, and the LO EBL has the weaker dust and stellar fields. Two other EBLs are considered here: a high dust/low stellar field and a low dust/high stellar field. Parameters of the CMBR and modified blackbodies are given in Table 1.

The intensity of the diffuse and unresolved γ -ray EBL from EGRET observations and analysis [23, 24] is shown in Figure 4. It is decomposed into contributions from blazars, separated into FSRQs and BL Lacs, and the superposed intensity from numerous faint sources where the γ rays are formed primarily by interactions of cosmic rays accelerated by supernovae in star-forming galaxies and by structure formation shocks in clusters of galaxies (reviewed in [26, 27]). The particle and radiation fields are connected because GZK effects of UHECRs with the EBL form cascade γ rays that contribute a truly diffuse component to the γ -ray EBL [25]. The intensity of this component is sensitive to the transition energy from galactic to extragalactic UHECRs and the formation rate of UHECR sources through time.

The analytic result for the energy-loss MFP of Fe with $A = 56$ on CMB photons is given by eq. (4) and labeled “analytic” in Figure 5. The accuracy is tolerable, but a more detailed calculation, also shown in Figure 5, is needed to draw more reliable conclusions. The numerical calculations for Fe treat photopion and photopair losses with the EBL as well as from universal

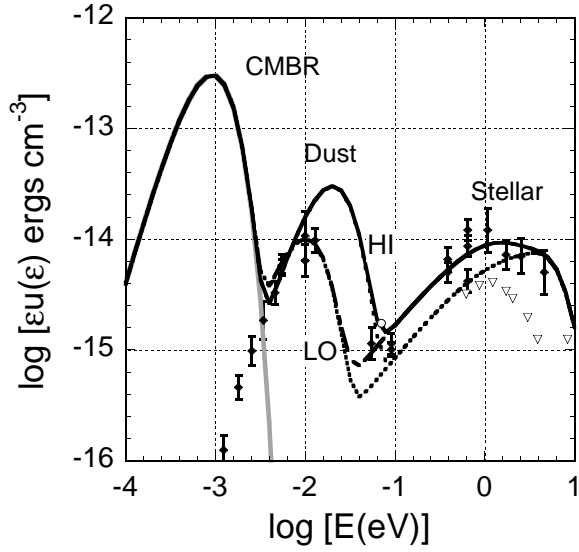


Figure 3. Ranges of EBL used in analysis. Data from Ref. [22]. The HI (LO) EBL refers to a high-(low-) intensity dust component and a high-(low-) intensity stellar component.

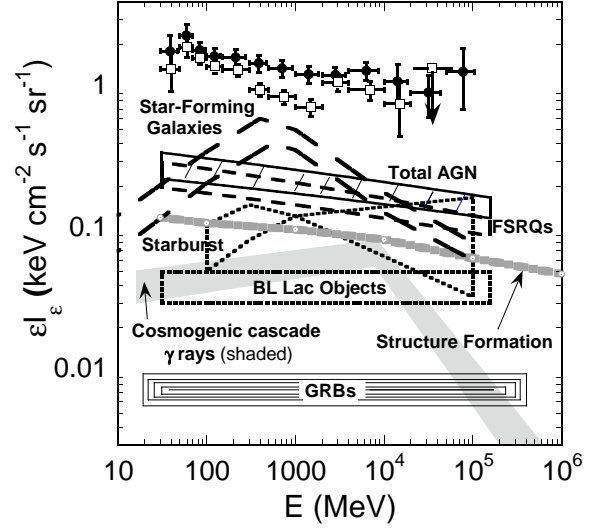


Figure 4. Decomposition of the diffuse/unresolved γ -ray background measured with EGRET [26]. Shaded region shows estimate for cascade γ -rays induced by UHECRs formed by sources evolving as AGNs [25].

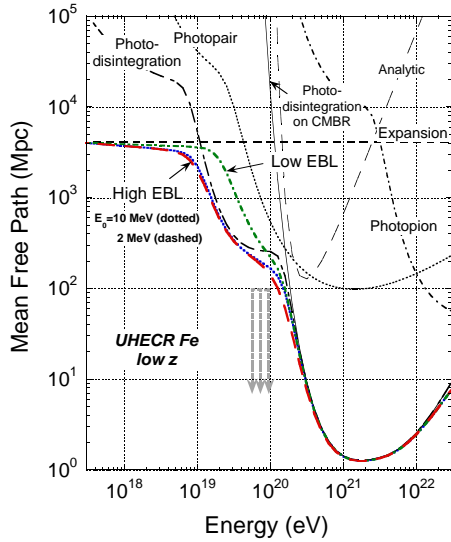


Figure 5. Effective energy-loss mean-free-path of Fe in LO and HI EBLs, with the effective photodisintegration energy-loss MFP calculated according to the prescription of Ref. [17].

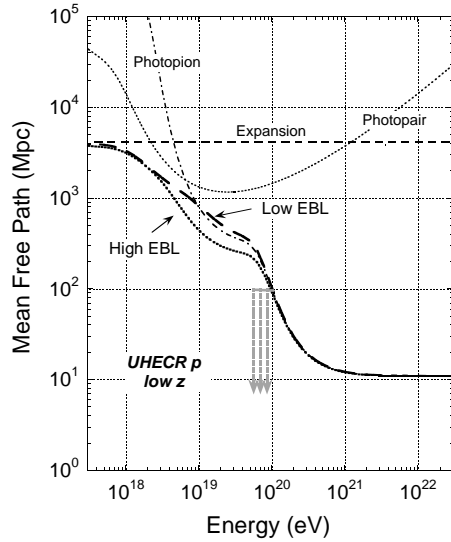


Figure 6. Effective energy-loss mean-free-path of UHECR protons in LO and HI EBLs shown in Fig. 3.

expansion (the Hubble radius is ≈ 4160 Mpc at the present epoch), with the photodisintegration, photopair, and photopion components shown separately for the HI EBL. The total energy loss MFP is also shown for the LO EBL. (See also [28, 29].) The distances from which we should expect to detect 60 – 100 EeV Fe range from ≈ 200 Mpc to 150 Mpc.

Fig. 6 shows the energy-loss MFP of UHECR protons in the LO and HI EBLs. The MFPs, which include photopion, photopair and expansion losses, range for the HI EBL from 200 to 100 Mpc for energies ranging from 60 to 100 EeV, respectively (similar to the values for UHECR Fe). Unless there was a deficit of UHECR sources between $\approx 100 - 200$ Mpc, or an enhanced pathlength due to strong, $\gtrsim 10^{-10}$ G intergalactic magnetic fields, it is difficult to account for unless UHECR p and Fe comprise only a small fraction of the $\gtrsim 60 \times 10^{19}$ eV UHECRs detected with Auger.

How else to resolve the quandary that the UHECR proton and Fe MFPs are too long to be commensurate with the Auger data, so that the UHECRs cannot be protons or Fe? Possibly the Auger detector is not properly calibrated, though it is unlikely to be off by more than $\approx 20\%$ compared to the factor of ≈ 2 needed. For instance, Berezhinsky [30], using the dip energy seen most clearly in an E^3I plot (see Fig. 1) as a fiducial, and multiplying by an energy calibration factor 1.2, 0.75, 0.83, and 0.625 for Auger, AGASA, Akeno and Yakutsk data, respectively, puts the various data sets in agreement with each other. Watson [33] argues that there are $\approx 19\%$ and 11% errors in the Auger energy calibration at 10^{17} and 10^{20} eV, respectively, so the correction factor for Auger is $\lesssim 1.2$. If this is true, then only a few percent of the $\gtrsim 6 \times 10^{19}$ eV UHECRs could be protons.

Let us provisionally accept that the Auger clustering results and the calculations presented here require that $\gtrsim 60$ EeV UHECRs are depleted in p and Fe (a full Monte Carlo simulation is required to remove remaining uncertainties). Some models, in particular, the neutral beam model that Armen Atoyan and I developed (for blazars, see [14], and for GRBs, see [31]) were based on the acceleration of protons to $\gtrsim 10^{20}/\Gamma$ eV energies in the shocked fluid frame, where Γ is the flow Lorentz factor. Photopion processes make an escaping neutron and γ -ray beam. If protons do not make up a large fraction of the $\gtrsim 10^{19.6}$ eV UHECRs, then this model no longer has to contend with the difficulty of accelerating protons to such high energies. On the other hand, this or any other model must be able to accelerate ions to ultra-high energies and get them from the accelerator into intergalactic space with the requisite emissivity.

Which ions? Again accepting the approximate integral meaning of an energy-loss MFP, Figures 7 and 8 show that UHECR ions up to Ne ($A = 20$) or at most Mg ($A = 24$) would effectively lose their energy within ≈ 100 Mpc. An abundance of UHECRs in light ions gives the most economical explanation of the Auger results. If correct, then composition analyses of 60 – 100 EeV UHECR data will give an average atomic mass number $\langle A \rangle \lesssim 24$ ($\langle \ln A \rangle \lesssim 3.2$), and probably in the range $\langle A \rangle \lesssim 20$. This prediction can be compared with Fig. 10 in Watson [33], giving the measured energy dependence of $\langle \ln A \rangle$ using the the QGSJETII-03 model. According to our calculations, the anisotropy of $\cong 60$ EeV UHECRs with $d_{max} \lesssim 50 - 100$ Mpc could only originate from nuclei with $2 \lesssim \langle \ln A \rangle \lesssim 3$ (the lower limit is not firm, and depends on source type).

Let us return to the question of the EBL. The dust EBL primarily attenuates $\gtrsim 4$ TeV photons and the stellar EBL primarily attenuates $\lesssim 4$ TeV. The LO and HI EBLs can be used to calculate $\tau_{\gamma\gamma}$ up to redshifts $z \approx 0.25$ where cosmic evolutionary processes start to change the EBL energy density compared to the present. The exponential attenuation factor $\exp(\tau_{\gamma\gamma})$ as a function of photon energy E for different redshifts is plotted in Figure 9. We can make a cut defined by $\exp(\tau_{\gamma\gamma}) = 10$ (or any other number, for that matter) to define a relationship between redshift and photon energy (the relation defined by $\tau_{\gamma\gamma}(z, E) = 1$ is sometimes referred to as the ‘‘Fazio-Stecker relation [34]’’; see also [35]) Here we make the cut defined by $\exp(\tau_{\gamma\gamma}) = 10$ to give the obscuration energy E_{osc} as a function of obscuration redshift z_{osc} , shown in Fig.

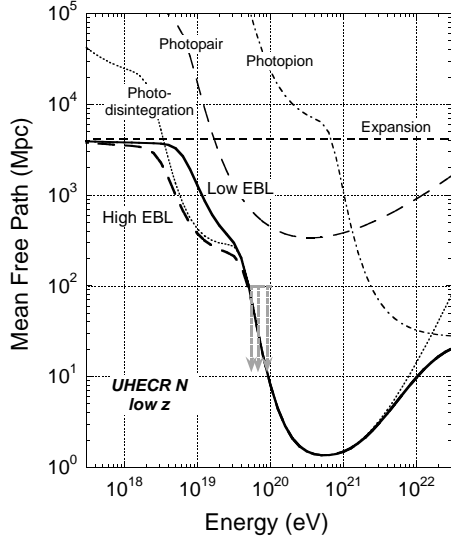


Figure 7. As in Fig. (5), for UHECR N.

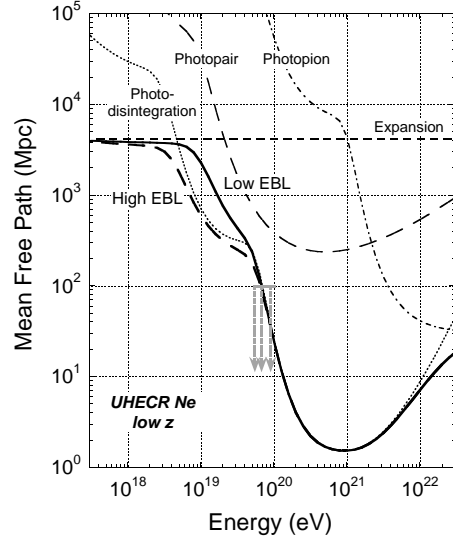


Figure 8. As in Fig. (5), for UHECR Ne.

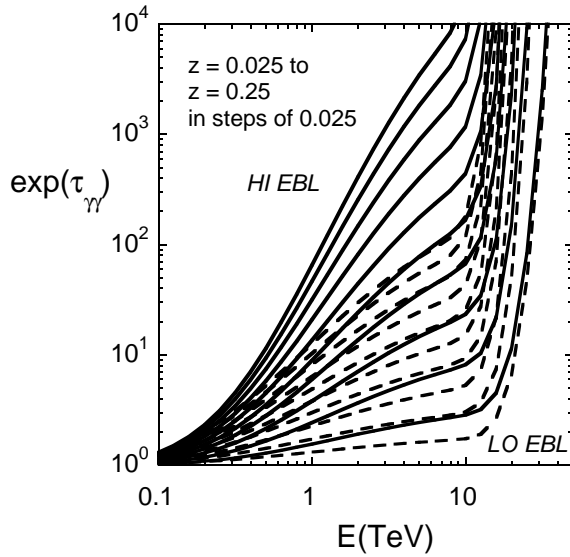


Figure 9. The factor $\exp(\tau_{\gamma\gamma})$ at different redshifts for the LO and HI EBLs shown in Fig. 3, as a function of photon energy E .

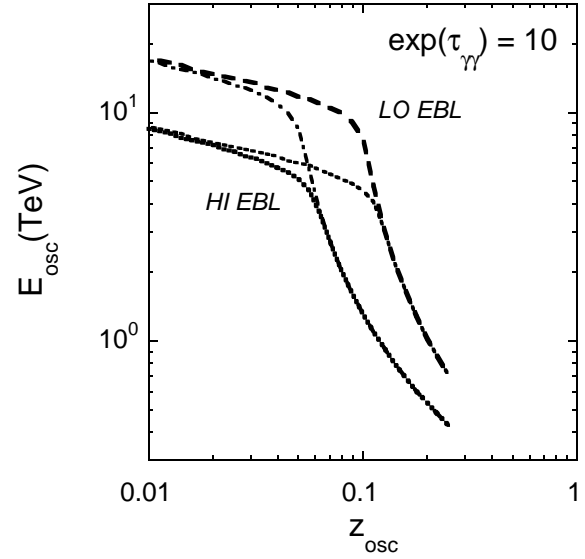


Figure 10. Relation between the obscuration energy E_{osc} and obscuration redshift z_{osc} defined by $\exp(\tau_{\gamma\gamma}) = 10$ for various high and low dust and stellar EBLs.

10. This figure is not however very useful for comparison with observational data, because the highest measured energies of photons depend upon telescope sensitivity, and variable source spectral brightness. Nevertheless, the dust component forms an opaque screen to photons with $E \gtrsim 7$ TeV and $\gtrsim 15$ TeV for the high and low dust EBL at the redshift $z \approx 0.03$ of Mrk 421 and Mrk 501. Significant detection of ≈ 8 TeV from Mrk 421 [36, 37] and Mrk 501 [38], and of $\gtrsim 10$ TeV photons from 1ES 0229+200 [39] ($z = 0.14$) suggests that the EBL intensity at $\sim 10 - 100 \mu\text{m}$ is smaller than given by the high dust EBL.

We now ask why the sources of UHECRs should be enriched in medium mass (C – Ne) nuclei. Refs. [15, 16] discusses various scenarios for accelerating UHECRs with significant ion content in GRB environments, including capturing supernova shell material by a jetted relativistic wind, external shock capture of circumburst material, and hypernovae [40]. We favor the hypothesis [41] that an external shock is important during the prompt and early afterglow phases of a GRB. GRBs formed by core collapse of C or O Wolf-Rayet stellar progenitors would be surrounded by a wind enriched in these light elements that could be captured and accelerated to ultra-high energies. This could be accomplished by 1st- or 2nd-order Fermi processes at the shock formed by the interaction of a relativistic wind with the surrounding medium.

For blazars and radio galaxies that propel intermittent winds to form internal shocks, the composition of UHECRs would depend on the makeup of the matter accreting onto supermassive black holes. If near-Solar metallicities occur [32], then proton acceleration would have to be suppressed, perhaps by a gyroresonant mechanism, and the medium mass ions would have to be processed through the black hole environment without breakup due to spallation or photodisintegration.

4. Discussion

The clustering result reported [1] by the Auger Collaboration is a major discovery, anticipated by Stanev, Biermann, Lloyd-Evans, Rachen, and Watson [5] in 1995. In the earlier study, Northern hemispheric data from Haverah Park, AGASA, Volcano Ranch, and Yakutsk with 73 (27), 25 (7), 13 (5), and 32 (3) events above 20 (40) EeV, respectively, and with zenith angles smaller than 45° were analyzed. The average and rms angular distances of the arrival directions of UHECRs from the supergalactic plane were calculated, after correcting for exposure. Compared to an isotropic source flux, a statistical enhancement towards the supergalactic plane at the 2.5 – 2.8 σ level was found for arrival directions of events with $E > 40$ EeV. The supergalactic plane runs through the Virgo Cluster at ≈ 20 Mpc, and contains an assortment of radio galaxies such as M87, Cen A and NGC 315, and the starburst galaxies M82 and NGC 253. Stanev et al. [5] argue that their analysis supports the hypothesis that radio galaxies are the sources of UHECRs accelerated, for example, in the inner jets or at the knots or hot spots of radio galaxies. Supporting this contention is the analysis of Shaver and Pierre [42] showing harder integral source count distributions of extragalactic radio sources at large spectral fluxes toward the supergalactic plane in the 408 MHz 1 Jy southern hemisphere Molonglo catalog, and clustering of sources in the 2.7 GHz 2 Jy Wall and Peacock catalog [43] towards the supergalactic plane. This clustering conforms with the association of UHECR arrival directions with radio sources in the supergalactic plane.

By comparison, the Auger team [1, 2] uses the VCV catalog [6] consisting of 85,221 quasars, 1122 BL Lac objects and 21,737 active galaxies (including 9628 Seyfert 1s). Quoting Véron-Cetty and Véron, “This [VCV] catalogue should not be used for any statistical analysis as it is not complete in any sense, except that it is, we hope, a complete survey of the literature.” The associations between the arrival directions of UHECRs and directions to nearby AGN in the VCV catalog may only reflect that both the AGNs in the VCV catalog and the sources of UHECRs within $\approx 50 - 100$ Mpc are preferentially found toward the supergalactic plane, and that the large number of sources in the VCV catalog gives an apparent stronger underlying association than would be found if a smaller catalog, such as the Wall and Peacock catalog, were used. Associations made with a mixed catalog are more likely to be spurious, and the removal of statistical biases in such analyses are challenging. Correlating UHECR arrival directions with flux-limited surveys of sources with relatively complete redshift information is the only reliable way of identifying the source population(s) of UHECRs in the absence of high-energy neutrino detection from these sources or discovery of anomalous γ -ray signatures in radio galaxies and GRBs with GLAST.

A concern expressed recently [45, 46] is that although some of the UHECRs observed with Auger are associated with the direction toward Cen A, none seem to originate from the Virgo cluster center of our supergalaxy in the direction of M87. The lower exposure of Auger toward M87, by a factor of 3 compared the exposure to Cen A [2], and the Northern Hemisphere detection of UHECRs that could be associated with Virgo [5, 44] could ameliorate this issue. Ref. [46] suggests that if all UHECRs are C, then the short energy-loss MFP of C would mask M87 and explain preferential detection of Cen A. But our calculations show that the effective energy loss MFP of UHECR C with $E \cong 60$ EeV is ≈ 50 Mpc, within which M87, at a distance of ≈ 18 Mpc, falls. The MFP of UHECR He at 60 – 100 EeV is $\sim 3 - 5$ Mpc, and so could restrict arrival directions to Cen A.

The dip energy, viewed as a consequence of photopair effects on UHECR protons [30] either from GRBs [47] or AGNs [48], could involve photodisintegration and photopair energy losses of ions interacting with photons of the EBL. There is also the possibility, again, that there is a deficit of UHECR sources between ≈ 100 and ≈ 300 Mpc. Whether this is true depends on source type, in particular whether UHECRs originate from specific classes of GRBs or AGNs.

In summary, the Auger team has opened charged particle astronomy by correlating the anisotropic arrival directions of $\gtrsim 60$ EeV UHECRs with AGNs located within ≈ 75 Mpc. Calculations presented here of the effective energy-loss MFP support an origin of UHECR ions in light nuclei with $A \lesssim 24$. The conclusion following from this analysis is that detection of UHECR clustering is most easily understood if most UHECRs are mainly light nucleons. The identification of the actual underlying source population must use complete (at least at high, $|b| \gtrsim 10^\circ$, galactic latitude) flux-limited catalogs.

Acknowledgments

I would like to thank Justin Finke and Soebur Razzaque for many useful conversations and for comments on the paper, Isabelle Grenier for sharing her presentations, and Venya Berezhinsky and the organizers of the Topics in Astroparticle and Underground Physics TAUP 2007 Conference in Sendai for the opportunity to attend the conference and visit Japan. This work is supported by the Office of Naval Research, NASA *GLAST* Science Investigation DPR-S-1563-Y, and NASA *Swift* Guest Investigator Grant DPR-NNG05ED411.

References

- [1] Auger Collaboration, 2007, *Science*, vol.318, p.939-943 (9 November 2007)
- [2] The Pierre Auger Collaboration 2007, ArXiv e-prints, 712, arXiv:0712.2843
- [3] Dermer, C. D. 2007, ArXiv e-prints, 711, arXiv:0711.2804, in 30th ICRC, Mérida, Yucatan, Mexico
- [4] Dermer, C. D., & Menon, G., “High Energy Radiation from Black Holes: γ rays, cosmic rays, and neutrinos,” to be published by Princeton University Press.
- [5] Stanev, T., Biermann, P. L., Lloyd-Evans, J., Rachen, J. P., & Watson, A. A. 1995, *Physical Review Letters*, 75, 3056
- [6] Véron-Cetty, M.-P., & Véron, P. 2006, *Astronomy and Astrophysics*, 455, 773
- [7] Bird, D. J., et al. 1995, *Astrophysical Journal*, 441, 144
- [8] Greisen, K. 1966, *Physical Review Letters*, 16, 748
- [9] Zatsepin, G. T. and Kuz'min, V. A. 1966, *JETP Lett.* 4, 78
- [10] Yamamoto, T., & for the Pierre Auger Collaboration 2007, ArXiv e-prints, 707, arXiv:0707.2638
- [11] HiRes Collaboration 2007, ArXiv Astrophysics e-prints, submitted to PRL, arXiv:astro-ph/0703099
- [12] Unger, M., Engel, R., Schüssler, F., Ulrich, R., & Pierre AUGER Collaboration 2007, *Astronomische Nachrichten*, 328, 614, arXiv:0706.1495v1
- [13] Watson, A. A. 2006, *Nuclear Physics B Proceedings Supplements*, 151, 83
- [14] Atoyan, A. M., & Dermer, C. D. 2003, *Astrophysical Journal*, 586, 79
- [15] Wang, X.-Y., Razzaque, S., & Mészáros, P. 2007, ArXiv e-prints, 711, arXiv:0711.2065, *ApJ*, in press
- [16] Murase, K., Ioka, K., Nagataki, S., & Nakamura, T. 2008, ArXiv e-prints, 801, arXiv:0801.2861
- [17] Puget, J. L., Stecker, F. W., & Bredekamp, J. H. 1976, *Astrophysical Journal*, 205, 638
- [18] Stecker, F. W., & Salamon, M. H. 1999, *Astrophysical Journal*, 512, 521

- [19] Karakula, S., & Tkaczyk, W. 1993, *Astroparticle Physics*, 1, 229
- [20] Anchordoqui, L. A., Beacom, J. F., Goldberg, H., Palomares-Ruiz, S., & Weiler, T. J. 2007, *Physical Review D*, 75, 063001
- [21] Waxman, E., & Bahcall, J. 1999, *Physical Review D*, 59, 023002
- [22] Hauser, M. G., & Dwek, E. 2001, *Annual Review of Astronomy and Astrophysics*, 39, 249
- [23] Sreekumar, P., et al. 1998, *Astrophysical Journal*, 494, 523
- [24] Strong, A. W., Moskalenko, I. V., & Reimer, O. 2004, *Astrophysical Journal*, 613, 962
- [25] Kalashev, O. E., Semikoz, D. V., & Sigl, G. 2007, ArXiv e-prints, 704, arXiv:0704.2463
- [26] Dermer, C. D. 2007, in *The Multi-Messenger Approach to High-Energy Gamma-Ray Sources*, eds. J. M. Paredes, O. Reimer, and D. F. Torres (New York: Springer), 127
- [27] Kneiske, T. M. 2007, ArXiv e-prints, 707, arXiv:0707.2915
- [28] Harari, D., Mollerach, S., & Roulet, E. 2006, *Journal of Cosmology and Astro-Particle Physics*, 11, 12
- [29] Hooper, D., Sarkar, S., & Taylor, A. M. 2007, *Astroparticle Physics*, 27, 199
- [30] Berezhinsky, V. 2008, ArXiv e-prints, 801, TAUP 2007 Conference, arXiv:0801.3028
- [31] Dermer, C. D., & Atoyan, A. 2003, *Physical Review Letters*, 91, 071102
- [32] Anders, E., & Grevesse, N. 1989, *Geochimica et Cosmochimica Acta*, 53, 197
- [33] Watson, A. A. 2008, ArXiv e-prints, 801, arXiv:0801.2321
- [34] Fazio, G. G., & Stecker, F. W. 1970, *Nature*, 226, 135
- [35] Kneiske, T. M., Bretz, T., Mannheim, K., & Hartmann, D. H. 2004, *Astronomy and Astrophysics*, 413, 807
- [36] Fossati, G., et al. 2007, ArXiv e-prints, 710, arXiv:0710.4138
- [37] Yadav, K. K., et al. 2007, *Astroparticle Physics*, 27, 447
- [38] Samuelson, F. W., et al. 1998, *Astrophysical Journal Letters*, 501, L17
- [39] Aharonian, F., et al. 2007, *Astronomy and Astrophysics*, 475, L9
- [40] Wang, X.-Y., Razzaque, S., Mészáros, P., & Dai, Z.-G. 2007, *Physical Review D*, 76, 083009
- [41] Dermer, C. D., & Mitman, K. E. 2004, *Astronomical Society of the Pacific Conference Series*, 312, 301
- [42] Shaver, P. A., & Pierre, M. 1989, *Astronomy and Astrophysics*, 220, 35
- [43] Wall, J. V., & Peacock, J. A. 1985, *MNRAS*, 216, 173
- [44] Cunningham, G., Lloyd-Evans, J., Pollock, A. M. T., Reid, R. J. O., & Watson, A. A. 1980, *Astrophysical Journal Letters*, 236, L71
- [45] Gorbunov, D., Tinyakov, P., Tkachev, I., & Troitsky, S. 2007, ArXiv e-prints, 711, arXiv:0711.4060
- [46] Fargion, D. 2008, ArXiv e-prints, 801, arXiv:0801.0227
- [47] Wick, S. D., Dermer, C. D., & Atoyan, A. 2004, *Astroparticle Physics*, 21, 125
- [48] Aloisio, R., Berezhinsky, V., Blasi, P., Gazizov, A., Grigorieva, S., & Hnatyk, B. 2007, *Astroparticle Physics*, 27, 76

